Turkish Journal of Civil Engineering, 2026, 1-21, Paper 841, ***Research Article***

Pozzolanic Reactivity of Calcareous Low-Grade Calcined Clays

Oğul Can YEŞILYURT[1]
Ömer Faruk KALKAN[2*]
Serkan TÜRK[3]
İsmail Özgür YAMAN[4]

ABSTRACT

Clays have played a fundamental role in human development, from early use in pottery and construction to modern applications in advanced ceramics, pharmaceuticals and environmental remediation. Their properties, combined with their abundance, make them an indispensable material for meeting today's engineering challenges, reinforcing their importance for sustainable development and technological innovation. With the increasing urgency of carbon emission reduction, the use of calcined clays to reduce the carbon footprint of the cement sector has become a near-term focus. It is well known that heating kaolinitic clays to certain temperatures increases their reactivity, making them suitable for cement and concrete applications, such as the use of metakaolin in high performance concrete and limestone calcined clay cements for reduced carbon intensity. Of particular interest, however, is the calcination of under-utilized low-grade clays that are not used in such production processes and do not meet the stringent requirements of high-quality ceramics, paper coatings or refractories. When properly processed, these low-grade clays may also exhibit pozzolanic reactivity, enhancing the durability and performance of cementitious systems while simultaneously reducing environmental impact and offering economic advantages. This study evaluated the pozzolanic reactivity of eight different clays, actively employed and readily sourced by Turkish cement plants from their existing deposits, following thermal activation at 600°C and 800°C. The relationship between the presence of kaolinite,

Note:
- This paper was received on September 5, 2025 and accepted for publication by the Editorial Board on December 19, 2025.
- Discussions on this paper will be accepted by September 31, 2026.
- https://doi.org/10.18400/tjce.1778319

1 Middle East Technical University, Department of Civil Engineering, Ankara, Türkiye
ogulcanyyt@gmail.com - https://orcid.org/0000-0002-5958-726X

2 Başkent University, Department of Civil Engineering, Ankara, Türkiye
Middle East Technical University, Department of Civil Engineering, Ankara, Türkiye
farukkalkan@baskent.edu.tr - https://orcid.org/0000-0001-9291-1773

3 Turkish Cement Manufacturers' Association R&D Laboratory, Ankara, Türkiye
serkant@turkcimento.org.tr - https://orcid.org/0009-0008-5458-9515

4 Middle East Technical University, Department of Civil Engineering, Ankara, Türkiye
ioyaman@metu.edu.tr - https://orcid.org/0000-0001-6489-6852

* Corresponding author

montmorillonite, illite, and calcite, and the resulting pozzolanic reactivity was analyzed. Thermogravimetric analysis/differential thermal analysis (TGA/DTA), X-ray diffraction (XRD), X-ray fluorescence (XRF), and particle size distribution (PSD) analyses were performed on the clays for characterization. The results showed that samples with higher clay mineral content exhibited lower strength in the absence of calcite. In other words, it was ultimately demonstrated that even clays with lower clay mineral content can be effectively utilized as SCMs through thermal activation, with the presence of calcite further enhancing their reactivity.

Keywords: Clay calcination, clay composition, calcareous clays, strength activity index, sustainable cement production.

1. INTRODUCTION

The detrimental effects of global warming have led to an increased focus on improving the sustainability of cement production [1,2]. The negative impact of cement production on global warming is largely due to the significant CO_2 emissions from the calcination of limestone during clinker production and the energy required to achieve high temperatures through coal combustion [3,4]. In this context, Türkiye has one of the largest cement production capacities worldwide, and the sector represents a significant contributor to national CO_2 emissions. As global and regional carbon reduction targets become increasingly stringent, reducing emissions from cement production has also become a critical priority in Türkiye. Supplementary cementitious materials (SCMs) have emerged as a viable option to reduce clinker use and improve the sustainability of cement systems through the incorporation of various additives [5,6]. Research has shown that substituting various types of SCMs for cement leads to improved sustainability, performance and cost-effectiveness [5,7-9]. Natural pozzolanic materials, such as calcined clays, have also been identified as a promising source of SCM with great potential for the cement industry [6,10]. Although clays have been used throughout human history, from ancient pottery and construction to modern applications in various industries, their use is now finding a renewed and critical role in sustainable construction through calcination. Clay deposits are abundant and readily available, unlike industrial byproducts such as fly ash and blast furnace slag, which may become scarce with increased recycling and alternative energy sources [11]. Also, clay formation continues repeatedly [12,13]. However, the behavior of clays can vary significantly depending on their mineral composition, organic matter and moisture content, among other factors. Therefore, a thorough investigation of the properties of clays before and after calcination is necessary to optimize their use in cement systems and consistently reduce costs, energy consumption, and emissions.

The use of clays as SCMs after thermal activation is not new [6,14], but recent technological advances (e.g., nuclear magnetic resonance) have provided a better understanding of the degradation, such as dihydroxylation, that occurs during the calcination of clay minerals and its effect on strength [6,15–17]. During the calcination of clay minerals, the hydroxyl bonds are broken, revealing the aluminate present in the mineral structure. The location of the aluminate and silicate in the clay mineral is critical to reactivity: Silicates in the mineralogical structure of clay are relatively more resistant to high temperatures and therefore retain their arrangement to some extent after calcination, making it difficult for the trapped aluminate to

be released [15]. The mineral structure of kaolinite is such that it releases the most aluminate when hydroxyl groups are removed, making it the most reactive clay mineral after calcination [15,18,19]. Similarly, illite mineral, which has the strongest silicate framework, gains reactivity after calcination [15,20,21]. In a cementitious system, the ratios of CaO (C), Al_2O_3 (A), and SiO_2 (S) determine the binding phases, and a ternary phase diagram has been developed, as shown in Figure 1. When the appropriate C, A, and S ratios are achieved in a cement system containing calcined clay and sufficient water (H_2O, H), the C-A-S-H gel is formed, which has binding properties and contributes to strength [16,22–24]. Normally, in a system consisting only of cement and calcined clay, most of the C is attributed to the portlandite ($Ca(OH)_2$ or CH) formed during cement hydration [25]. In this case, C causes a bottleneck effect in the formation of the C-A-S-H phase, and the presence of calcite can alleviate this bottleneck effect. As a result of understanding this situation, the use of limestone powder together with calcined clay in cement replacement has become crucial, and some optimized technologies, such as limestone-calcined clay cement (LC^3), have been developed as a low-carbon cement [15,26–29].

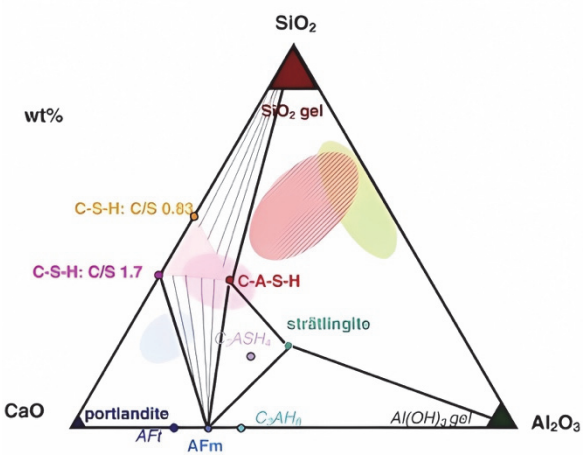

Figure 1 - Ternary phase diagram of the hydrates in a cementitious system [15]

A standard LC^3 mix contains 45% cement clinker, 30% calcined clay, 15% limestone and 5% gypsum [27]. Studies [15,27,30,31] have shown that mixtures containing 40% kaolinite can reach the strength of ordinary Portland cement in 7 days. However, the mineralogical composition of the clay, i.e., the amount and existence of different clay minerals present, also has a significant effect on the performance of the blend. Moreover, the amount of calcite in the clay should also be considered when adjusting the optimum ratio of calcined clay to limestone.

It has been shown that incorporating up to 50% calcined marl, which contains both calcite and clay, can reach compressive strengths comparable with OPC [32–34]. Furthermore, Bahhou et al. [24] has revealed that, hydration process of marl incorporates the aluminates into C-S-H gels, forming C-A-S-H gels, enhancing the microstructure. Furthermore, residual calcite supports the formation of carboaluminate. Similarly, C-S-H formation is also

encountered in a geopolymer microstructure when calcite-rich clays were used [35]. The ash obtained by burning at 750-950°C of calcite-rich oil shale, which has high organic content, solidifies without any cement addition [36]. Thermal treatment of clay-limestone or siliceous limestone, i.e. calcareous clayey materials, results in formation of a β-belite, which is a hydraulic phase [37]. As a conclusion, materials rich in calcite and clay exhibit self-cementing (latent hydraulic) behavior due to their balanced composition [21].

A significant challenge in the cement sector is the use of high-quality clays, such as kaolinite, which necessitates separate grinding from limestone due to their different grindability, thereby raising energy and cost burdens [38]. Furthermore, the high demand for high-quality clays in industries like paper and ceramics, where color control is critical, drives up their price [39]. To address these issues, using calcareous clays offers the potential to utilize lower-grade clays and streamline processing. Therefore, this study aims to explore the supplementary cementitious material (SCM) potential of low-grade or calcareous clays, actively employed and readily sourced by Turkish cement plants from their existing deposits, following thermal activation at 600°C and 800°C. The relationship between the presence of different clay minerals, such as kaolinite, montmorillonite and illite, and their calcite content, and the resulting pozzolanic reactivity will be analyzed to provide insight into the potential for LC^3.

2. EXPERIMENTAL PROGRAM

2.1. Characterization of Clay Minerals

As mentioned earlier, the clays used in this study are obtained from the existing clay deposits of Turkish cement plants. The geographical distribution of the cement plants and the clay sources are illustrated in the map shown in Figure 2. These clays are labeled as Clay A to H

Figure 2 - Locations of the clays together with the cement plants of Türkiye (adopted by [40])

(Figure 3). Rietveld analysis was performed by the R&D laboratories of the Turkish Cement Manufacturers' Association on the clays and the results are presented in Table 1. As observed in that table, the analyzed samples have different mineral compositions: Except for Clay C, ***kaolinite*** is present in almost all clays in varying amounts (2 to 28 %), and Clays A, F and H contain moderate (> 20%) amounts of ***kaolinite***. Clays D, F and H contain moderate amounts of ***montmorillonite***. While all clays contain some ***illite***, Clays A, C, and G contain moderate amounts (> 15%). Clay B is the only clay that contains a significant amount of ***nontronite*** (34.7%). Clays E and H contain moderate amounts of ***clinochlore*** (> 15%). In addition to these clay minerals, Clays C, E, B, D, F and A contain varying amounts (6 to 44 %) of ***calcite***. Other minerals, such as ***quartz*** and ***albite,*** are also present in most of the clays.

Figure 3 - Clays used in this study, which are in their raw form

Table 1 - Mineralogical composition of clays (%)

Mineral	Clay A	Clay B	Clay C	Clay D	Clay E	Clay F	Clay G	Clay H
Kaolinite	27.7	2.6	0.2	11.7	2.3	28.3	14.0	23.0
Montmorillonite	8.0	2.9	-	33.5	-	27.9	-	16.0
Illite	15.7	0.8	17.1	4.6	5.0	1.6	16.0	8.0
Clinochlore	6.5	-	-	-	21.0	-	-	16.0
Nontronite	-	34.7	-	-	-	-	-	-
Calcite	5.9	29.0	43.8	14.8	31.0	12.9	-	0.9
Quartz	23.0	17.2	13.2	14.5	19.1	17.0	38.0	29.0
Albite	11.1	7.8	20.2	13.1	8.0	9.9	-	6.0
Muscovite	-	-	-	1.1	-	2.5	13.0	-
Dolomite	-	-	-	-	3.5	-	7.0	-
Palygorskite	-	-	-	-	10.0	-	-	-

Mineral	Clay A	Clay B	Clay C	Clay D	Clay E	Clay F	Clay G	Clay H
Anorthite	-	-	-	6.7	-	-	-	-
Vermiculite	-	-	-	-	-	-	6.0	-
Hematite	-	-	-	-	-	-	6.0	-
Microcline	-	5.0	-	-	-	-	-	-
Sanidine	-	-	4.6	-	-	-	-	-
Rutile	2.1	-	-	-	-	-	-	-

Besides the XRD analysis, XRF analysis was also conducted (Table 2) to verify the chemical composition of clays as obtained from the Rietveld analysis. Due to the high quartz and clay mineral content, all clays contain significant amounts of SiO_2 and Al_2O_3. As expected, clays with high calcite content also had high CaO content. Loss on ignition (LoI) increases with the amount of CaO due to decarbonization of calcite at high temperatures. Although Clays A and H have low CaO contents, they have high LoI values. This can be explained by the presence of clinochlore, which releases chlorine gas at high temperatures, causing this mass loss.

Table 2 - Chemical composition of clays

Clay	LoI	SiO_2	Al_2O_3	Fe_2O_3	CaO	MgO	SO_3	Na_2O	K_2O
A	5.8	57.6	17.3	9.3	1.2	2.8	-	0.8	2.7
B	18.7	41.8	12.6	8.3	12.3	4.9	0.1	0.3	1.8
C	18.6	40.2	10.8	6.3	17.4	3.3	0.1	0.6	1.3
D	11.3	52.0	13.4	5.5	11.5	2.4	0.2	1.3	1.5
E	18.9	41.8	9.9	6.4	14.3	5.7	0.1	0.8	1.3
F	13.1	44.7	13.3	10.3	10.5	6.7	0.1	0.8	1.7
G	5.1	52.3	18.7	16.9	1.4	2.4	-	-	4.1
H	6.9	52.2	21.9	11.1	1.9	2.6	-	0.7	3.1

Thermal analyses were also performed on all clay samples using TGA/DTA to investigate weight changes with temperature and to determine potential calcination temperatures (Figure 4). The results suggested free water evaporation between 50-200 °C, combustion of volatile organic materials between 100-200 °C, and release of chemically bound water between 200-300 °C. In addition, peaks between 300-450 °C were suggested to correspond to hydroxide decomposition. In addition, the results indicate that the kaolinite calcined between 450-600 °C and illite decomposed between 600-850 °C. Clays with little or no calcite content seemed to show smaller weight changes, while those with significant calcite content seemed to show the disappearance of calcite peaks between 600°C and 800°C. This may indicate that calcite decarbonization may have occurred between 700-750°C, releasing CO_2. As a result of these analyses for all clays 600 and 800 °C were selected for the two calcination temperatures.

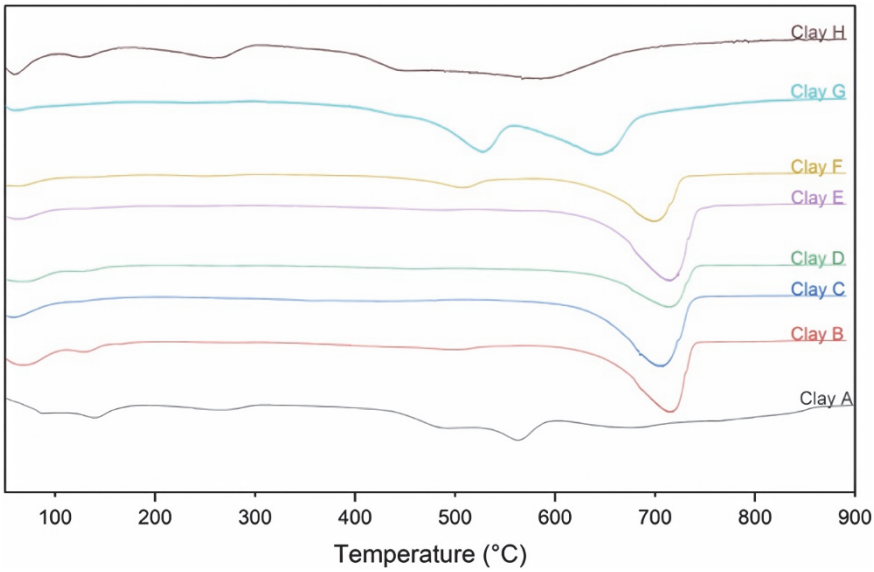

Figure 4 - Temperature versus derived weight curves of the clays

2.2. Calcination of the Clays

Based on some preliminary studies, the clays were ground for 60 minutes after being quartered in their raw state and dried to remove moisture. The ground clays were then sieved through a 75 µm mesh and subjected to static calcination using a furnace at a heating rate of 10°C/min to the target temperature (600°C or 800°C), and held at the target temperature for 60 minutes to confirm the decomposition of the clay minerals after calcination, as determined by preliminary calcination trials. The calcined clays were subjected to X-ray diffraction (XRD) analysis to confirm this decomposition. The particle size distribution (PSD) analysis was performed on the clays before and after calcination (Figure 5). As can be seen in Figure 5(a), all clays had a similar fineness prior to calcination, with the exception of Clay D, which was coarser. After calcination at 800 °C, all the clays were still fine enough with the majority of the clays being smaller than 75 microns. However, as observed from Figure 5(b), the variation in fineness was more pronounced, with the average 50% pass size varying from 5 microns to 13 microns. In literature, the size reduction during calcination was explained by thermally-induced physical cracking of the coarser particles, and the size increase was attributed to sintering of the clay minerals [41,42]. On the other hand, it should be noted that laser-based PSD measurements require the assumption of a specific refractive index for each tested material [43]. In addition, potential agglomeration associated with the use of the dry dispersion method, as well as the inherent heterogeneity of the clay materials, may also bring some uncertainty into the PSD results. Nevertheless, all calcined clays exhibit sufficient fineness to support effective pozzolanic reactions.

The XRD patterns in Figure 6 show the disappearance of peaks associated with clay minerals after calcination at 800°C. This observation indicates that the clay minerals have undergone decomposition and transformed into amorphous phases, indicating a possible thermal

activation process. However, the sharp and intense peaks of the quartz phase, present in significant amounts in all clays, dominate the XRD patterns and largely mask the broad humps typically associated with the amorphous phase [44], weak and diffuse humps remain discernible, suggesting the presence of an amorphous product. In addition, the disappearance of calcite peaks after calcination also indicates that calcite decarbonization occurs, releasing CO_2 at elevated temperatures. Although, the decomposition of calcite may result in excessive free lime and may lead to undesired expansion [38], this can be mitigated in the cementitious system with the consumption of the portlandite in pozzolanic reactions. However, in the case of cement or blended cement formulations, the associated expansion should be explicitly verified through appropriate expansion or soundness testing.

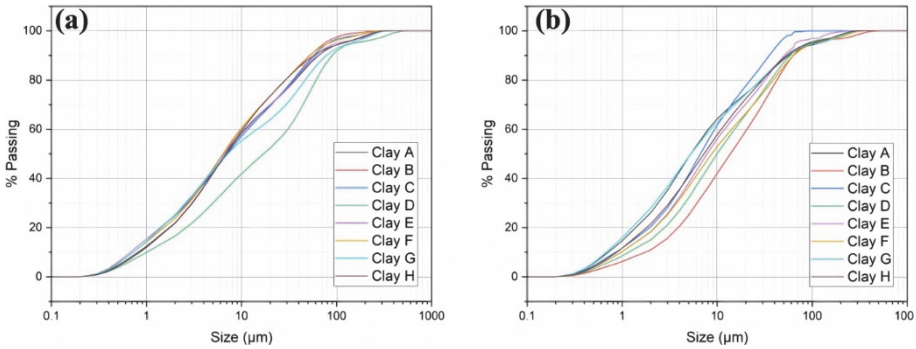

Figure 5 - PSD curves of clays a) uncalcined and b) calcined at 800 °C

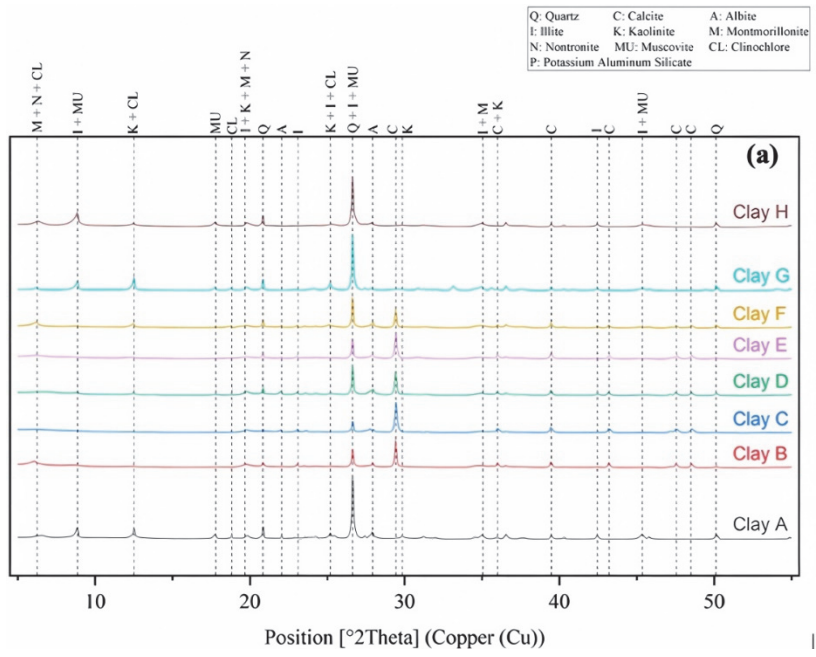

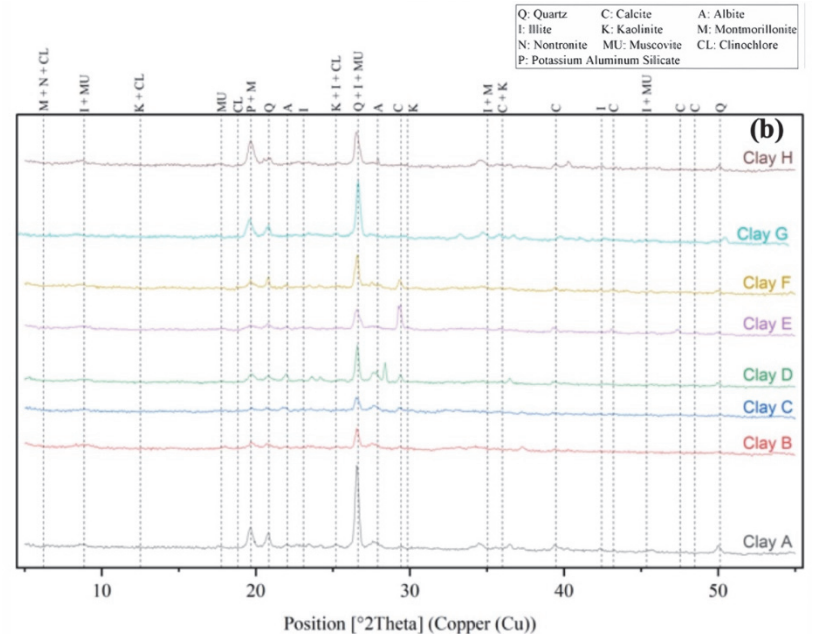

Figure 6 - XRD patterns of clays a) uncalcined and b) calcined at 800 °C

2.3. Pozzolanic Activity of the Calcined Clays

To assess the pozzolanic activity of the calcined clays, the strength activity index (SAI) of the calcined clays was determined from control and 20% cement replacement mortar samples prepared according to ASTM C311 and poured into 40x40x160 mm prismatic molds. Flow table tests were carried out on the mortar samples according to the ASTM C230 standard when water is added to the mortar mix to obtain a constant flow. The increase in water demand according to the Control mortar is shown in Table 3.

All mortar samples were cured in a lime-water solution at 20±2°C for 7, 28 and 90 days. At the end of each curing period, the compressive strength of the mortar samples was determined, and SAI at each age was calculated according to ASTM C311. The mean compressive strengths and corresponding coefficients of variation (CoV) of the mortar specimens are presented in Table 4.

Examining the SAI data presented in Figure 7(a), it can be seen that none of the clays showed sufficient strength development in the uncalcined state and that the incorporation of raw clays into cement blends reduced the strength by approximately 40% compared to the Control cement at all ages. It is, therefore, clear that at no age did the uncalcined clays meet the SAI requirement of 75% as defined by ASTM C 618.

On the other hand, when calcination was carried out at 600 °C, it is clear from Figure 7(b) that Clay C and D met the SAI requirement at all ages and Clays A, B and F only met it at 90 days. When the calcination temperature was increased to 800 °C, as shown in Figure 7(c), the SAI of the clays generally increased. Clays B, C, D, E and F fulfilled this requirement at all ages and Clay A only at 90 days of age. Clays G and H were not successful at any age.

Table 3 - Increase in water demand of mortars due to 20% clay replacement

Clay	No Calcination	Calcined at 600 °C	Calcined at 800 °C
A	+13.1%	+8.1%	+8.7%
B	+38.2%	+10.8%	+10.8%
C	+21.7%	+10.2%	+10.8%
D	+15.9%	+7.0%	+7.6%
E	+21.0%	+9.6%	+11.5%
F	+17.0%	+9.5%	+8.3%
G	+10.8%	+12.0%	+9.5%
H	+20.4%	+14.6%	+12.1%

Table 4 - Compressive strength test results

Calcination Temperature	Clay Label	7-Day		28-Day		90-Day	
		Strength (MPa)	CoV (%)	Strength (MPa)	CoV (%)	Strength (MPa)	CoV (%)
-	Control	40.6	2.8	51.6	3.8	55.8	5.3
No Calcination	A	25.8	4.8	28.4	3.2	41.0	4.2
	B	18.5	1.4	23.0	1.9	25.7	2.0
	C	24.8	1.5	33.0	2.1	39.8	1.3
	D	26.5	2.3	33.9	2.2	37.5	2.0
	E	24.2	3.2	30.5	1.4	32.6	1.7
	F	24.7	1.0	31.6	1.2	34.6	3.0
	G	27.0	3.4	35.3	1.4	36.0	2.6
	H	22.4	3.1	30.0	1.7	33.3	1.5
600°C	A	29.7	2.6	32.2	1.3	38.8	5.0
	B	29.7	2.0	37.4	2.7	40.5	2.9
	C	33.1	1.2	45.7	1.5	49.6	3.7
	D	31.2	2.8	44.6	4.2	50.0	2.2
	E	29.2	3.1	35.6	1.1	41.9	2.1
	F	31.8	0.6	35.4	2.0	43.1	2.8
	G	30.0	1.5	36.3	1.3	37.3	2.1
	H	26.0	1.7	35.0	2.5	38.1	1.8

Calcination Temperature	Clay Label	7-Day		28-Day		90-Day	
		Strength (MPa)	CoV (%)	Strength (MPa)	CoV (%)	Strength (MPa)	CoV (%)
800°C	A	28.6	3.1	34.7	2.3	44.2	2.0
	B	32.6	1.9	45.1	2.3	48.3	2.5
	C	33.1	1.2	50.4	1.6	59.4	2.0
	D	32.9	2.4	48.1	1.5	53.3	3.0
	E	33.5	1.7	45.0	2.7	49.8	1.8
	F	34.1	2.0	42.9	1.1	45.7	1.9
	G	30.9	0.9	37.4	0.9	38.6	1.8
	H	27.7	2.2	35.0	1.3	39.7	2.2

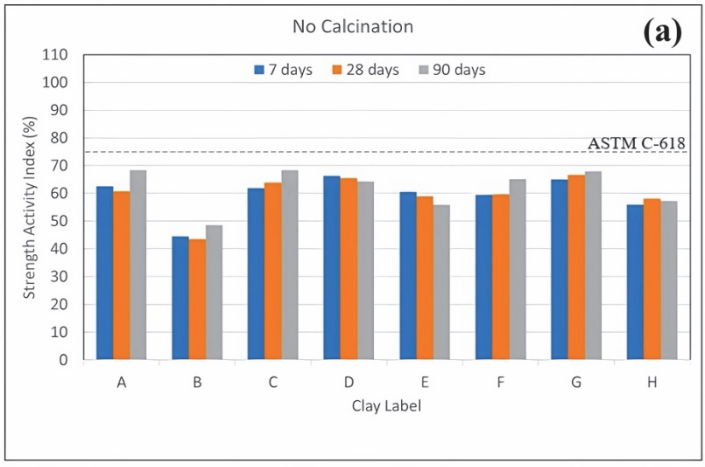

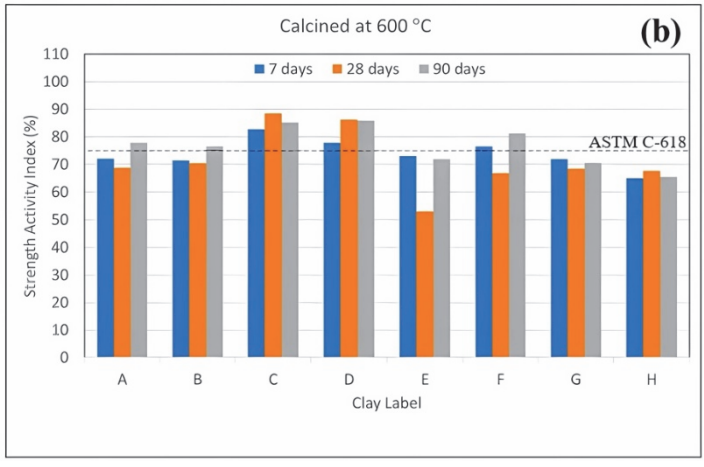

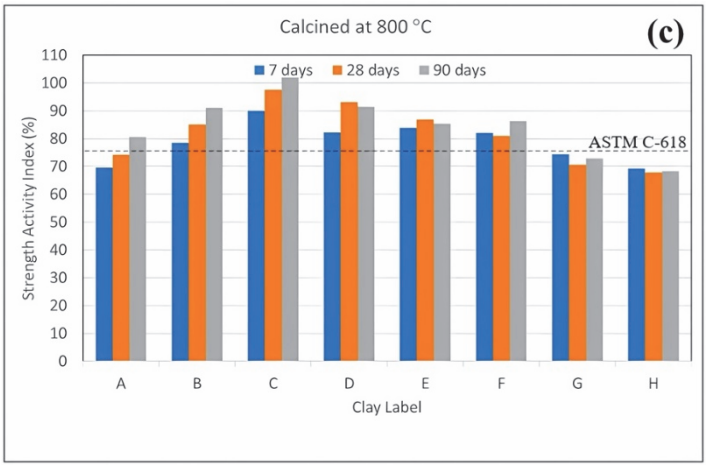

Figure 7 - SAI of clays (a) uncalcined (b) calcined at 600 °C and (c) calcined at 800 °C

To identify correlations between strength activity index (SAI), and the chemical and mineralogical composition and particle size distribution (PSD) of the clays, Pearson correlation analysis was conducted using SPSS software. The significance level (p-value), reflecting the strength of the correlation, was evaluated. Lower p-values indicate stronger correlations, and a threshold of $p < 0.01$ or $p < 0.05$ was used to determine statistical significance.

Table 5 - Pearson correlation test results of SAI for clays calcined at 800 °C

	Correlation Parameter	7-day SAI		28-day SAI		90-day SAI	
		Pearson correlation	p-value	Pearson correlation	p-value	Pearson correlation	p-value
Chemical Composition	SiO_2	-0.796*	0.018	-0.639	0.088	-0.646	0.083
	Al_2O_3	-0.889**	0.003	-0.880**	0.004	-0.866**	0.005
	Fe_2O_3	-0.612	0.107	-0.801*	0.017	-0.733*	0.039
	CaO	0.951**	0.000	0.927**	0.001	0.885**	0.004
	MgO	0.418	0.303	0.219	0.601	0.278	0.505
Mineralogical Composition	Total Clay$^{\xi}$	-0.640	0.074	-0.542	0.165	-0.504	0.135
	Kaolinite	-0.646	0.084	-0.678	0.065	-0.591	0.123
	Montmorillonite	-0.003	0.994	0.048	0.910	-0.009	0.950
	Illite	-0.162	0.701	-0.157	0.710	-0.101	0.812
	Calcite	0.851**	0.007	0.860**	0.006	0.869**	0.005
	Quartz	-0.733*	0.039	-0.854**	0.007	-0.870**	0.005
	Albite	0.655	0.078	0.780*	0.023	0.819*	0.013

Particle Size	**d(0.1)**	0.225	0.592	0.376	0.358	0.403	0.322
	d(0.5)	0.266	0.525	0.384	0.347	0.396	0.332
	d(0.9)	-0.435	0.282	-0.379	0.354	-0.332	0.421

Note: Sample size (N) is 8 for each parameter

* Correlation is significant at the 0.05 level (2-tailed).

** Correlation is significant at the 0.01 level (2-tailed).

ξ The total clay content represents the sum of all identified clay minerals – namely the kaolinite group (kaolinite), mica group (illite and muscovite), smectite group (montmorillonite, nontronite, and vermiculite), and chlorite group (clinochlore) – as quantified by Rietveld analysis

Considering that the fineness of all clays was comparable, as also demonstrated by Pearson's correlation analysis (Table 5), it is evident that the chemical composition of the clays plays an essential role in the SAI test results. When analyzing the relationship between each clay mineral type and the SAI test results of calcined clays at 800 °C, specifically focusing on the three clay minerals - kaolinite, montmorillonite, and illite - it is observed that there is no direct correlation between the SAI test results at both 28 and 90 days (Table 5 and Figure 8). Moreover, for kaolinite there seems to be a weak and negative correlation. This apparent discrepancy is explained by the fact that, although metakaolin is inherently highly reactive, the SAI in blended cement systems is influenced by the overall mineralogical and chemical composition of the calcined clays. In the clays studied, calcite-derived CaO plays a more influential role in enhancing hydration and strength development than kaolinite content alone.

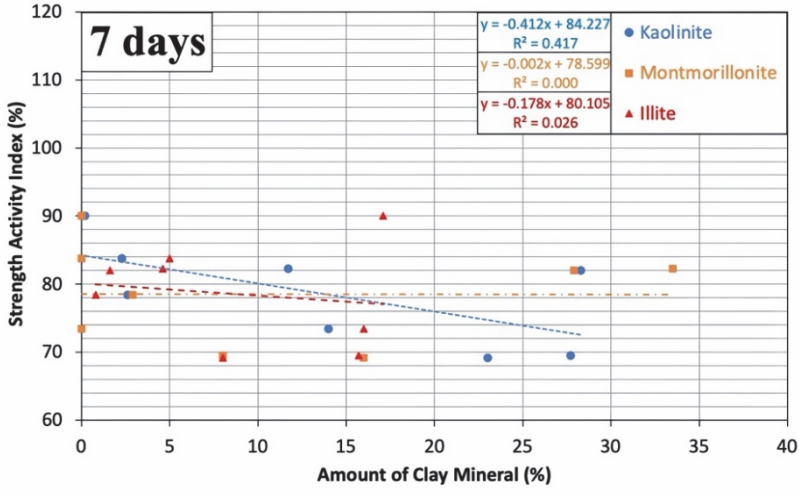

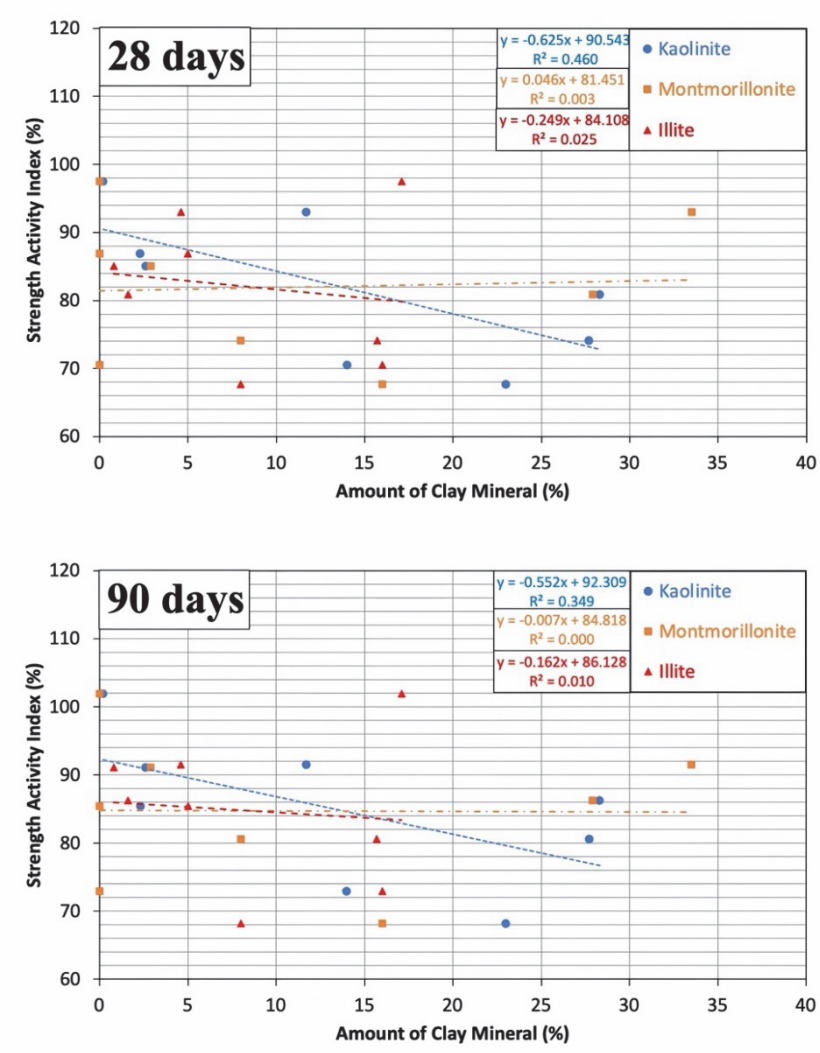

Figure 8 - Influence of clay mineral type on SAI for clays calcined at 800 °C

Figure 9 shows the influence of mineralogical composition on the strength activity index (SAI) of clays calcined at 800 °C at 7, 28, and 90 days. The total clay mineral content (Figure 9a) exhibits a weak negative correlation with SAI, indicating that overall clay content alone does not govern strength performance. Similarly, Quartz content (Figure 9b) is negatively correlated with SAI due to its largely inert nature, while albite content (Figure 9c) exhibits a moderate positive correlation with SAI.

On the other hand, when the same analysis is performed with respect to calcite content, it is clear that there is a strong correlation between the calcite amount present in the clays and the

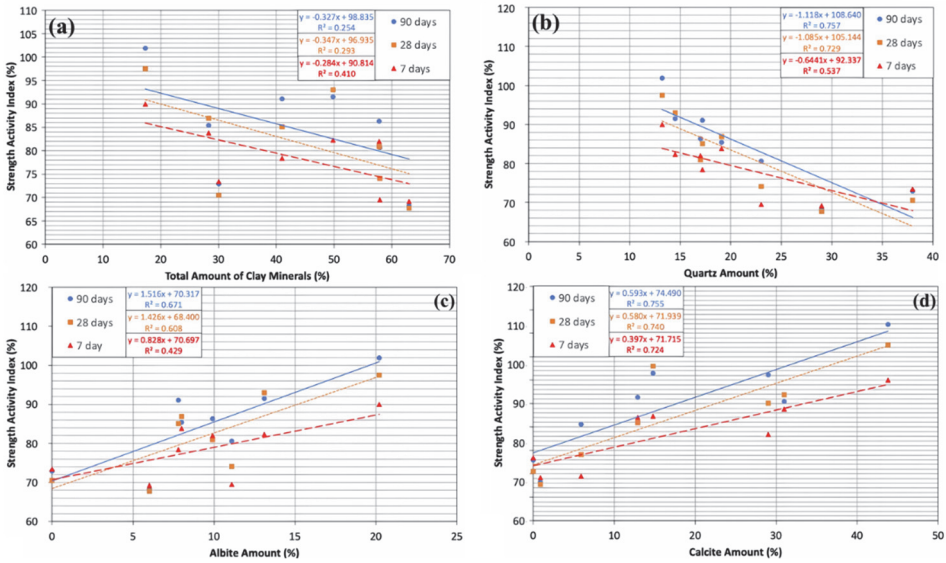

Figure 9 - Influence of (a) all clay minerals, (b) quartz, (c) albite, and (d) calcite on SAI for clays calcined at 800 °C

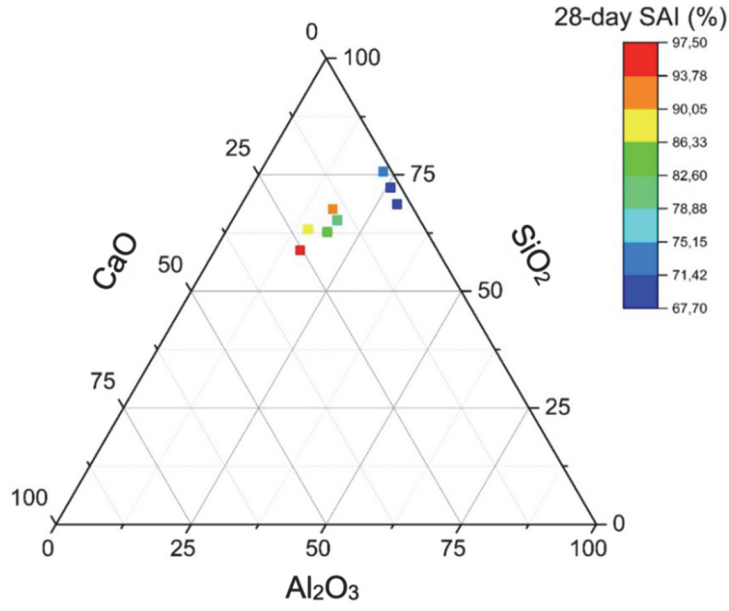

Figure 10 - Effects of Chemical Composition on the SAI of Calcined Clays

SAI. The presence of calcite in clays was therefore found to be beneficial, with clays having a higher calcite content showing improved strength performance, possibly due to overcoming of the bottleneck effect. The ternary diagram (Figure 10) provides substantial evidence supporting this effect. The abundance of CaO in the system has been shown to increase the tendency for the formation of hemicarboaluminate, monocarboaluminate and C-A-S-H phases, thereby altering the hydration kinetics and overcoming the bottleneck effect. The denser microstructure is associated with reduced porosity and enhanced mechanical performance, attributable to the increased volume of hydration products.

2.4. Analysis of Hydration Products

To assess the hydration characteristics, XRD analysis was performed **on selected samples based on their overall performance,** including cement pastes incorporating clays A (lower overall performance), C (higher overall performance), and F (moderate overall performance), each calcined at 800 °C, as well as a control cement paste with a 20% cement replacement, all prepared at normal consistency. After setting, cement pastes were cured for 28 days in

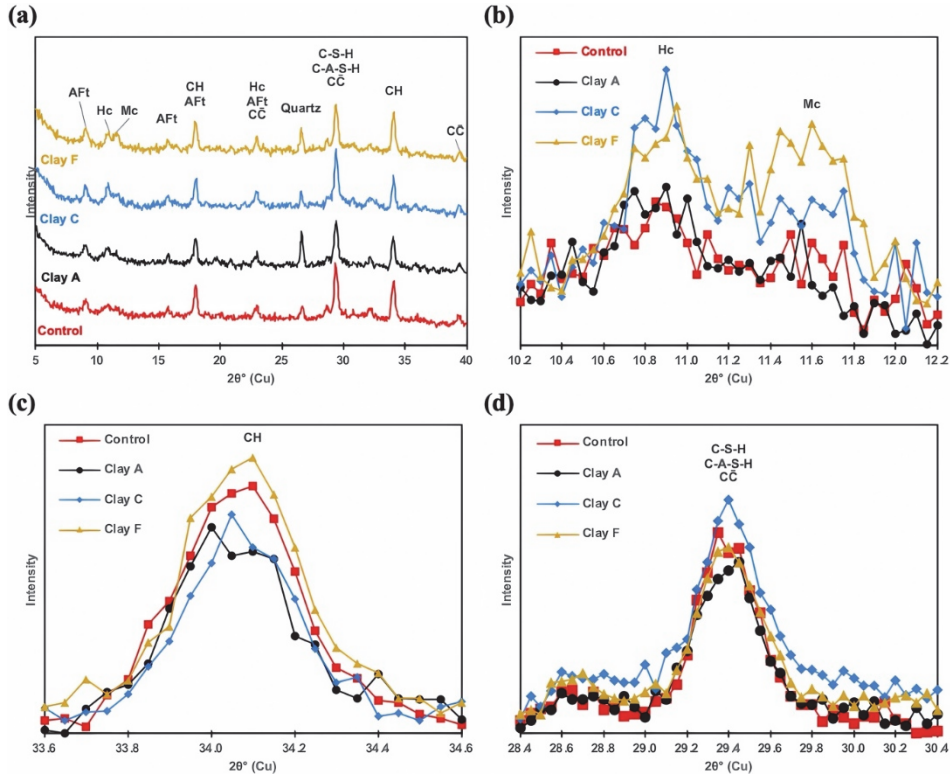

Figure 11 - (a) XRD analysis of cement pastes selected clays and comparison of (b) hemicarboaluminate (Hc), monocarboaluminate (Mc), (c) Portlandite (CH), (d) C-S-H,

water and ground under 75 μm maximum grain size. The XRD analysis demonstrated that replacing cement with calcined clays induced microstructural changes, given in Figure 11(a). Specifically, each clay type resulted in the formation of hemicarboaluminates and monocarboaluminates, which enhanced the cement's mechanical properties. Conversely, the quantities of Portlandite, C-S-H, and C-A-S-H exhibited variations depending on the clay used.

The Portlandite peak around 34.15° 2θ is given in Figure 11(c). The amount of Portlandite reduces in Clay A and C, and increases in Clay F. Portlandite in the hardened cement paste originates from two sources: as a hydration product of Portland cement and from the initial calcite present. During the calcination calcite is decomposed to CaO, as Figure 6 shows, subsequently in the matrix turns into Portlandite reacting with water. The decrease in Portlandite of Clay A is due to replacement of cement and decrease in hydration products. However, the reduction of Portlandite peak in Clay C, having the highest calcite amount, indicates that Portlandite is consumed by the calcined clay via pozzolanic reaction. The SAI of Clay C relates with this pozzolanic activity. The calcite amount of Clay F (%12.9) increase the Portlandite peak due to partial decomposition. As shown in Figure 11(d), although the amount of calcite is less than in Clay C, the Portlandite peak is longer, which can be attributed to the fact that the pozzolanic reactions did not occur as efficiently as in Clay C, as evidenced by the SAI results. Comparison of C-S-H and C-A-S-H gels, also support that pozzolanic reaction products is formed more abundantly in Clay C, F, and A, respectively, related to their SAIs.

3. CONCLUSION

The aim of this study is to investigate the supplementary cementitious material (SCM) potential of low-grade or calcareous clays after thermal activation. For this purpose, eight clays actively used by Turkish cement plants and readily sourced from their existing deposits are calcined at two different temperatures (600°C and 800°C) and characterized by various test methods. Later, the pozzolanic activity of the calcined clays is determined by the strength activity index (SAI) of the calcined clays.

The results show that kaolinite, illite and montmorillonite are the most common clay minerals present in the clays obtained from Turkish cement plants, with clinochlore and nontronite also present in some clays. TGA/DTA analysis shows an endothermic peak between 700-750°C, which is more pronounced in clays with higher calcite content, indicating decarbonation of calcite. XRD results show that the calcite peaks disappear in most clays after calcination at 800°C, probably due to calcite decarbonation.

Most clays are unable to meet the requirement of 75% SAI at 7 or 28 days, but Clay C, D, and F calcined at 600°C and Clay B, C, D, E, and F calcined at 800°C are able to meet the requirement. A direct correlation is found between calcite content and SAI results, indicating the importance of calcite in the reactivity of the calcined clays. Clay C, with the highest calcite content, exceeds 100% SAI at 90 days, while Clay A, G, and H could not show sufficient SAI due to low calcite content.

Overall, the study provides valuable insights into the characteristics of clays obtained from Turkish cement plants after calcination, including their mineral composition, changes in

physical properties, and performance as cement substitutes. The results highlight the potential of the calcined clays to be used as a clinker substitute, with calcite content and other mineralogical factors influencing their reactivity. Further research is warranted to explore the potential of these clays in a ternary LC^3 blends and other applications in the cement industry.

References

[1] T. S. Ledley, E. T. Sundquist, S. E. Schwartz, D. K. Hall, J. D. Fellows, and T. L. Killeen, "Climate change and greenhouse gases," Eos, Transactions American Geophysical Union, vol. 80, no. 39, pp. 453–458, Sep. 1999, doi: 10.1029/99EO00325.

[2] Framework Convention on Climate Change, "Report of the Conference of the Parties on its twenty-first session," Paris, Jan. 2016.

[3] F. Pacheco Torgal, S. Miraldo, J. A. Labrincha, and J. De Brito, "An overview on concrete carbonation in the context of eco-efficient construction: Evaluation, use of SCMs and/or RAC," Constr Build Mater, vol. 36, pp. 141–150, Nov. 2012, doi: 10.1016/J.CONBUILDMAT.2012.04.066.

[4] R. Feiz, J. Ammenberg, L. Baas, M. Eklund, A. Helgstrand, and R. Marshall, "Improving the CO2 performance of cement, part I: utilizing life-cycle assessment and key performance indicators to assess development within the cement industry," J Clean Prod, vol. 98, pp. 272–281, Jul. 2015, doi: 10.1016/J.JCLEPRO.2014.01.083.

[5] J. Duchesne, "Alternative supplementary cementitious materials for sustainable concrete structures: a review on characterization and properties," Waste Biomass Valorization, vol. 12, no. 3, pp. 1219–1236, Mar. 2021, doi: 10.1007/s12649-020-01068-4.

[6] M. Tokyay, "Cement and concrete mineral admixtures," Cement and Concrete Mineral Admixtures, pp. 1–305, Apr. 2016, doi: 10.1201/B20093/CEMENT-CONCRETE-MINERAL-ADMIXTURES-MUSTAFA-TOKYAY/RIGHTS-AND-PERMISSIONS.

[7] S. Prakasan, S. Palaniappan, and R. Gettu, "Study of Energy Use and CO2 Emissions in the Manufacturing of Clinker and Cement," Journal of The Institution of Engineers (India): Series A, vol. 101, no. 1, pp. 221–232, Mar. 2020, doi: 10.1007/S40030-019-00409-4.

[8] F. Eren, M. Keskinateş, B. Felekoğlu, and K. Tosun Felekoğlu, "Mineral Katkı İkamesinin Kalsiyum Alümina Çimentolu Harçların Taze Hal ve Zamana Bağlı Sertleşmiş Hal Özelliklerine Etkileri," Turkish Journal of Civil Engineering, vol. 34, no. 3, pp. 139–162, May 2023, doi: 10.18400/TJCE.1288033.

[9] S. Çelik, S. B. İkizler, D. Aqra, and Z. Angin, "Using Sea Shell, Lime and Zeolite as Additives in the Stabilization of Expansive Soils," Turkish Journal of Civil Engineering, vol. 36, no. 3, pp. 21–37, May 2025, doi: 10.18400/TJCE.1464572.

[10] F. Massazza, "Pozzolanic cements," Cem Concr Compos, vol. 15, no. 4, pp. 185–214, Jan. 1993, doi: 10.1016/0958-9465(93)90023-3.

[11] World Business Council for Sustainable Development, "Cement Industry Energy and CO2 Performance: Getting the Numbers Right (GNR)," 2016.

[12] D. D. Eberl, "Clay mineral formation and transformation in rocks and soils," Philosophical Transactions of the Royal Society of London. Series A, Mathematical and Physical Sciences, no. A311, pp. 241–257, Jun. 1984, doi: 10.1098/RSTA.1984.0026.

[13] Y. Tardy, G. Bocquier, H. Paquet, and G. Millot, "Formation of clay from granite and its distribution in relation to climate and topography," Geoderma, vol. 10, no. 4, pp. 271–284, Dec. 1973, doi: 10.1016/0016-7061(73)90002-5.

[14] E. Chiotis, E. Dimou, G. Papadimitriou, and S. Tzoutzopoulos, "The study of some ancient and prehistoric plasters and watertight coatings from Greece," Archaeometry Issues In Greek Prehistory And Antiquity, 2001.

[15] R. Fernandez, F. Martirena, and K. L. Scrivener, "The origin of the pozzolanic activity of calcined clay minerals: A comparison between kaolinite, illite and montmorillonite," Cem Concr Res, vol. 41, no. 1, pp. 113–122, Jan. 2011, doi: 10.1016/J.CEMCONRES.2010.09.013.

[16] A. Tironi, M. A. Trezza, E. F. Irassar, and A. N. Scian, "Thermal Treatment of Kaolin: Effect on the Pozzolanic Activity," Procedia Materials Science, vol. 1, pp. 343–350, Jan. 2012, doi: 10.1016/J.MSPRO.2012.06.046.

[17] Y. A. Atalay, T. Aydin, Z. Başaran Bundur, P. Mokhtari, M. A. Gülgün, and Z. Lafhaj, "Optimization of Hybrid Microwave Curing Approach Based On the Performance of Metakaolin-Based Geopolymer Mortars," Turkish Journal of Civil Engineering, vol. 35, no. 6, pp. 47–64, Nov. 2024, doi: 10.18400/TJCE.1322047.

[18] J. Ambroise, M. Murat, and J. Péra, "Hydration reaction and hardening of calcined clays and related minerals V. Extension of the research and general conclusions," Cem Concr Res, vol. 15, no. 2, pp. 261–268, Mar. 1985, doi: 10.1016/0008-8846(85)90037-7.

[19] O. D. Huang et al., "Feasibility of using calcined clays and reclaimed coal ashes in binary and ternary cementitious systems," Journal of Building Engineering, vol. 95, p. 110186, 2024, doi: https://doi.org/10.1016/j.jobe.2024.110186.

[20] C. He, E. Makovicky, and B. Øsbæck, "Thermal stability and pozzolanic activity of calcined illite," Appl Clay Sci, vol. 9, no. 5, pp. 337–354, Feb. 1995, doi: 10.1016/0169-1317(94)00033-M.

[21] T. Danner, G. Norden, and H. Justnes, "The Effect of Calcite in the Raw Clay on the Pozzolanic Activity of Calcined Illite and Smectite," in Calcined Clays for Sustainable Concrete, S. Bishnoi, Ed., Singapore: Springer Singapore, 2020, pp. 131–138.

[22] B. Lothenbach, K. Scrivener, and R. D. Hooton, "Supplementary cementitious materials," Cem Concr Res, vol. 41, no. 12, pp. 1244–1256, Dec. 2011, doi: 10.1016/J.CEMCONRES.2010.12.001.

[23] M. Atkins, F. P. Glasser, and A. Kindness, "Cement hydrate phase: Solubility at 25°C," Cem Concr Res, vol. 22, no. 2–3, pp. 241–246, Mar. 1992, doi: 10.1016/0008-8846(92)90062-Z.

[24] A. Bahhou, Y. Taha, R. Hakkou, M. Benzaazoua, and A. Tagnit-Hamou, "Assessment of hydration, strength, and microstructure of three different grades of calcined marls derived from phosphate by-products," Journal of Building Engineering, vol. 84, p. 108640, 2024, doi: https://doi.org/10.1016/j.jobe.2024.108640.

[25] A. M. Dunster, J. R. Parsonage, and M. J. K. Thomas, "The pozzolanic reaction of metakaolinite and its effects on Portland cement hydration," J Mater Sci, vol. 28, no. 5, pp. 1345–1350, Mar. 1993, doi: 10.1007/BF01191976/METRICS.

[26] A. Alujas, R. S. Almenares, S. Betancourt, and C. Leyva, "Pozzolanic reactivity of low grade kaolinitic clays: Influence of Mineralogical Composition," Appl Clay Sci, vol. 108, pp. 94–101, May 2015, doi: 10.1016/J.CLAY.2015.01.028.

[27] K. L. Scrivener, V. M. John, and E. M. Gartner, "Eco-efficient cements: Potential economically viable solutions for a low-CO2 cement-based materials industry," Cem Concr Res, vol. 114, pp. 2–26, Dec. 2018, doi: 10.1016/J.CEMCONRES.2018.03.015.

[28] S. Barbhuiya, J. Nepal, and B. B. Das, "Properties, compatibility, environmental benefits and future directions of limestone calcined clay cement (LC3) concrete: A review," Journal of Building Engineering, vol. 79, p. 107794, Nov. 2023, doi: 10.1016/J.JOBE.2023.107794.

[29] X. Huang, Z. Huang, Y. Zhou, R. Hu, and B. Hu, "Life cycle assessment and cost analysis of LC3 concrete considering sustainability and uncertainty," Journal of Building Engineering, p. 111960, 2025, doi: https://doi.org/10.1016/j.jobe.2025.111960.

[30] A. Alujas, R. Fernández, R. Quintana, K. L. Scrivener, and F. Martirena, "Pozzolanic reactivity of low grade kaolinitic clays: Influence of calcination temperature and impact of calcination products on OPC hydration," Appl Clay Sci, vol. 108, pp. 94–101, May 2015, doi: 10.1016/J.CLAY.2015.01.028.

[31] B. Liu, X. Gu, H. Wang, J. Liu, M. L. Nehdi, and Y. Zhang, "Study on the mechanism of early strength strengthening and hydration of LC3 raised by shell powder," Journal of Building Engineering, vol. 98, p. 111422, 2024, doi: https://doi.org/10.1016/j.jobe.2024.111422.

[32] T. A. Østnor and H. Justnes, "Durability of mortar with calcined marl as supplementary cementing material," Advances in Cement Research, vol. 26, no. 6, pp. 344–352, 2014, doi: 10.1680/adcr.13.00040.

[33] Y. Akgün, "Behavior of Concrete Containing Alternative Pozzolan Calcined Marl Blended Cement," Periodica Polytechnica Civil Engineering, vol. 64, no. 4, pp. 1087–1099, Jan. 2020, doi: 10.3311/PPci.15122.

[34] W. Kurdowski and T. Baran, "Calcined marl as a potential main component of cement," Cement-Wapno-Beton = Cement Lime Concrete, vol. 27, no. 5, pp. 346–354, 2022, doi: 10.32047/CWB.2022.27.5.4.

[35] Y. Ettahiri et al., "Comparative study of physicochemical properties of geopolymers prepared by four Moroccan natural clays," Journal of Building Engineering, vol. 80, p. 108021, 2023, doi: https://doi.org/10.1016/j.jobe.2023.108021.

[36] P. Talviste, A. Sedman, R. Mõtlep, and K. Kirsimäe, "Self-cementing properties of oil shale solid heat carrier retorting residue," Waste Management and Research, vol. 31, no. 6, pp. 641–647, Mar. 2013, doi: 10.1177/0734242X13482033/ASSET/IMAGES/LARGE/10.1177_0734242X13482033-FIG3.JPEG.

[37] A. Gnisci, "Preliminary characterization of hydraulic components of low-temperature calcined marls from the south of Italy," Cem Concr Res, vol. 161, p. 106958, 2022, doi: https://doi.org/10.1016/j.cemconres.2022.106958.

[38] F. Zunino and K. Scrivener, "Increasing the kaolinite content of raw clays using particle classification techniques for use as supplementary cementitious materials," Constr Build Mater, vol. 244, p. 118335, May 2020, doi: 10.1016/J.CONBUILDMAT.2020.118335.

[39] H. H. Murray and U. by Staff, "Clays, Survey," Kirk-Othmer Encyclopedia of Chemical Technology, pp. 1–29, Apr. 2014, doi: 10.1002/0471238961.1921182204151302.a01.pub3.

[40] TCMA, "Üye Fabrikalar," https://www.turkcimento.org.tr/assets/site/images/map-of-factories-v2.jpg?ver=92032.

[41] S. Ferreiro, M. M. C. Canut, J. Lund, and D. Herfort, "Influence of fineness of raw clay and calcination temperature on the performance of calcined clay-limestone blended cements," Appl Clay Sci, vol. 169, pp. 81–90, Mar. 2019, doi: 10.1016/J.CLAY.2018.12.021.

[42] K. Cwik, M. Broström, K. Backlund, K. Fjäder, E. Hiljanen, and M. Eriksson, "Thermal Decrepitation and Thermally-Induced Cracking of Limestone Used in Quicklime Production," Minerals, vol. 12, no. 10, p. 1197, Oct. 2022, doi: 10.3390/MIN12101197/S1.

[43] J. C. Pachon, K. R. Kowalski, J. K. Butterick, and A. R. Bacon, "Quantified Effects of Particle Refractive Index Assumptions on Laser Diffraction Analyses of Selected Soils," Soil Science Society of America Journal, vol. 83, no. 3, pp. 518–530, May 2019, doi: 10.2136/SSSAJ2018.07.0274;JOURNAL:JOURNAL:26911027;REQUESTEDJOURNAL:JOURNAL:14350661;PAGE:STRING:ARTICLE/CHAPTER.

[44] C. N. Achilles et al., "Amorphous Phase Characterization Through X-Ray Diffraction Profile Modeling: Implications for Amorphous Phases in Gale Crater Rocks and Soils," 2018.